Nanoscale

REVIEW

View Article Online
View Journal

Cite this: DOI: 10.1039/d5nr04104j

Review on carbon-based materials for moisture-induced energy harvesting

Jing Tan,[a,b] Chen Tian,[c] Longtao Liu,[c] Yupeng Liu,[d] Jinyun Tan,[e] Qijun Li,*[c] Jianning Ding*[c] and Songnan Qu *[d]

Moisture-enabled electricity generation (MEG) is an emerging energy-harvesting technology that continuously generates electricity by interacting with ubiquitous ambient water vapor in a pollution-free manner. Its integrable and miniaturizable nature makes it a promising candidate for future scalable and decentralized energy systems. This comprehensive review examines the evolution of MEG devices, focusing on the underlying mechanisms of moisture-material interactions, particularly ion diffusion and streaming potentials. We also provide a detailed analysis of novel carbon-based hygroscopic materials by discussing their types, characteristics, and merits/drawbacks. Finally, we summarize recent advances in MEG applications across various fields.

Received 28th September 2025,
Accepted 30th November 2025

DOI: 10.1039/d5nr04104j

rsc.li/nanoscale

1. Introduction

With the continuing threat of the energy crisis and global warming caused by the increasing utilization of fossil energy, the development of sustainable and green energy has become particularly important.[1,2] Electricity, as an indispensable secondary energy source in modern society, has evolved into a primary driving force behind the rapid development of both society and the economy due to its extensive range of applications and widespread dissemination. For many years, researchers have explored the potential of generating electricity from various renewable natural resources, including solar, wind, hydro, tidal, geothermal, and biomass energy. Among these alternatives, hydropower has garnered widespread attention because of its exceptional stability and relatively high power output.[3,4]

[a]Institute of Technology for Carbon Neutralization, College of Physical Science and Technology, Yangzhou University, Yangzhou 225009, China. E-mail: liqijun@yzu.edu.cn,dingjn@yzu.edu.cn
[b]State Key Laboratory of Organic Electronics and Information Displays & Institute of Advanced Materials (IAM), Nanjing University of Posts & Telecommunications, 9 Wenyuan Road, Nanjing 210023, China
[c]School of Mechanical Engineering, Institute of Technology for Carbon Neutralization, Yangzhou University, Yangzhou 225009, China. E-mail: songnanqu@um.edu.mo
[d]Institute of Applied Physics and Materials Engineering (IAPME), University of MacauTaipa, Macau SAR 999078, China
[e]Department of Vascular Surgery, Huashan Hospital of Fudan University, Shanghai, P. R. China

Jing Tan

Jing Tan received her PhD degree from Beijing University of Chemical Technology in 2017 under the supervision of Prof. Dongmei Yue. In April 2024, she joined the Yangzhou University. Currently, she is the full professor in Yangzhou University. Her research interests focus on the synthesis and optical properties of carbon-based material and their applications in energy conversion and storage, anti-counterfeiting and optoelectronic.

Chen Tian

Chen Tian received his B.E. degree in 2024 from Yangzhou University. He is currently pursuing his M.S. degree at Yangzhou University under the joint supervision of Professor Qijun Li and Professor Jing Tan. His current research focuses on the preparation and application of moisture-enabled electricity generation devices and supercapacitors.

Conventional hydropower technology primarily focuses on energy conversion mechanisms associated with water phase transitions. It involves the conversion of the kinetic or potential energy of flowing water into electrical energy through mechanical devices. While hydropower presents distinct advantages, conventional hydropower technology inherently possesses certain limitations. Its implementation is critically dependent on regional water availability, typically confining development to areas with abundant water resources. Moreover, the substantial initial capital investment poses a major economic constraint on its broad deployment. Consequently, the global expansion of conventional hydropower technology is significantly impeded by the synergistic limitations of geographical availability and economic feasibility. As an emergent energy harvesting technology, moisture-enabled electric generation (MEG) has garnered significant attention in recent years due to its low cost (Fig. 1), high efficiency, and the absence of harmful byproducts. The ubiquitous presence of atmospheric water vapor[5] (Fig. 2a) and the environmentally friendly nature of the generation process confer exceptional adaptability to MEG across temporal, geographic, and environmental conditions.[6] Consequently, MEG technology holds substantial potential for future development.

In the 19th century, electrokinetic phenomena such as streaming potential were first observed when water flowed through narrow channels or crevices under a pressure gradient, providing a foundational basis for understanding electricity generation through nanomaterial–water interactions. In 2009, Galembeck[7] demonstrated that exposure to high relative humidity (RH) induces excess surface charges on materials including cellulose, hydrophilic particles, and even metals. Later termed hydroelectricity, this phenomenon has since been recognized as a critical mechanism for moisture-enabled energy conversion. In 2015, Qu and co-workers[8] successfully designed an oxidized graphene structure with an oxygen functional group concentration gradient, which enabled the generation of electrical power through humidity variations. The structure exhibited a rapid reaction to changes in relative humidity (RH), with its mechanism primarily involving charge transfer between adsorbed water molecules and the active layer materials, thereby producing free charges. Owing to the oxygen functional group concentration gradient, these free charges experience directional migration, ultimately resulting in a stable direct current (DC) output. These findings have sparked considerable academic interest in active layer materials and have accelerated the development of theoretical models for humidity-driven energy generation.[9] In particular, researchers refer to the charge transfer phenomenon between water molecules and active layer material molecules as the "hydrovoltaic effects".[10]

Comprehensive reviews on MEG technology have been scarce, primarily due to several major challenges in the field. These challenges include its relatively short development history and the lack of a systematic understanding of its underlying mechanisms, especially for the emerging carbon-based MEG devices. In this review, we first elucidate the fundamental working principles of MEGs. We then probe the interaction mechanisms between moisture and materials, focusing on ion diffusion and streaming potential. We also provide a critical analysis of novel carbon-based hygroscopic materials by assessing their types, properties, and trade-offs. Finally, we catalog recent advancements in MEG applications. We expect this review to catalyze further exploration and help expand the application landscape for moisture-powered devices in energy and sensing.

2. Mechanisms of electricity generation

The core of the MEG mechanism lies in the driving forces and pathways of charge migration. Migrating ions primarily originate from the electric double layer (EDL) effect at the water–solid interface or are driven by protons released from chemical

Longtao Liu

Longtao Liu received his B.E. degree in 2022 from Huaibei Normal University. He is currently pursuing his M.S. degree at Yangzhou University under the supervision of Professor Qijun Li. His current research focuses on the preparation and application of moisture-enabled electricity generation devices.

Yupeng Liu

Yupeng Liu obtained his bachelor's degree in chemistry from Hunan University in 2020 and completed his Ph.D. under the supervision of Prof. Qu Songnan in applied physics and materials engineering at the University of Macau in 2024. He currently acts as a postdoctoral fellow at the University of Macau. His research interests include the optical bandgap regulation of carbon dots, the afterglow luminescence of carbon dots, and their applications in biological imaging, lasers, information encryption, etc.

reactions between water molecules and functional groups (*e.g.*, –OH, –COOH) on the solid surface. Particularly within nanoscale confined spaces, the formation and evolution of the EDL critically influence charge separation efficiency. When the channel size approaches or falls below the Debye length, significant EDL overlap occurs, causing the ion distribution to deviate from Boltzmann statistics and form non-neutral ion-enriched regions, thereby enhancing the local electric field strength and altering ion migration behavior. Based on the physical nature of this charge migration, the MEG mechanism can be categorized into two primary types: the ion gradient diffusion mechanism and the streaming potential mechanism. The former is driven by the directed flow of water molecules within micro/nano-channels, which in turn drives the migration of ions along with the fluid flow. In contrast, the latter is driven by gradients in humidity or the concentration of oxygen-containing functional groups within the material, facilitating the diffusive migration of ions. Notably, these two mechanisms are not mutually exclusive. Under specific material architectures and environmental conditions (*e.g.*, when both humidity gradients and microchannel flows are present), they can synergistically interact to enhance the overall electrical output performance. In addition, electrochemical redox reactions, ion exchange in heterostructures, directional migration of hydrated hydrogen ions (H_3O^+), and interfacial capacitance effects are also often involved in the wet gas power generation process, which together constitute the diversity of mechanisms.

2.1 Ion gradient diffusion

As shown in Fig. 2b, the device consists of a pair of inert electrodes and a moisture-absorbing material layer rich in groups (*e.g.* –OH, –COOH, and –SO_3H).[23] Under a certain level of humidity, water molecules interact with the oxygen-containing functional groups of the hygroscopic layer, undergoing hydration to ionize a large number of hydrogen ions. Due to the asymmetric distribution of these oxygen-containing groups, the side with a higher concentration of groups ionizes more ions. Under the influence of the concentration gradient, ions migrate from regions of high concentration to those of low concentration, leading to an uneven charge distribution and ultimately establishing a potential difference. The intrinsic driving force of this process, namely the proton affinity and dissociation energy of different functional groups, can be quantitatively evaluated by density functional theory (DFT) calculations. For example, DFT simulations can reveal that –COOH has a lower proton dissociation barrier than –OH, which theoretically explains why carboxyl is a more effective proton source.

In 2015, Qu and co-workers first[8] realized moisture-enabled electricity generation using graphene oxide (GO) materials. In their experiment, they first compressed prepared GO into a sheet and applied a voltage across its ends to create a gradient distribution of oxygen-containing functional groups. Then, leveraging the hydrophilic nature of GO, at a certain humidity, water molecules adsorbed on its surface, forming ion transport channels, while also causing the surface oxygen-containing groups to ionize and release ionic charge carriers. The gradient distribution of functional groups induced the diffusion of charge carriers from the high-concentration end to the low-concentration end, thereby creating a voltage across the ends and enabling electrical output.

To construct an asymmetric distribution of functional groups, researchers typically must employ specific physicochemical methods[17] to pre-treat the materials; however, for materials that are difficult to process, there remains a certain degree of limitation.

2.2 Streaming potential

Flow potential refers to the electrokinetic phenomenon in which free charges migrate along the liquid–solid interface as a liquid passes through porous structures or micro/nano channels as shown in Fig. 2c. This phenomenon is also used to explain part of the power generation mechanism in MEG. When an electrolyte solution comes into contact with a

Jinyun Tan

Jinyun Tan, a Chief Physician and Professor at Fudan University Huashan Hospital, is a Harvard-certified clinical research scholar. He specializes in vascular and aortic surgeries, performing over 500 operations annually, with his dialysis access cases consistently ranking among the best in Shanghai. His research focuses on developing biodegradable vascular stents and advanced biomaterials, supported by national grants and resulting in numerous high-impact publications and patents. He has been recognized with awards including the Shanghai Medical Science Progress Award.

Qijun Li

Qijun Li is currently the professor in School of Mechanical Engineering, Institute of Technology for Carbon Neutralization, Yangzhou University, China. He received his PhD degree from Tsinghua University in 2018 under the supervision of Prof. Ming Zhou. His research interest is focused on the synthesis of carbon dots materials and the study of their optical and electrical properties.

charged insulating surface, the process is primarily influenced by electrostatic attraction and repulsion forces. Ions in the solution that carry a charge opposite to that of the surface approach and form a dense adsorption layer, while ions with the same charge as the surface form a diffusion layer in a more distant region; these two layers collectively constitute the "double layer" structure. In nanochannels, the overlap of the EDL significantly enhances solid–liquid interfacial interactions, potentially altering the magnitude or even reversing the polarity of the zeta potential, thereby critically influencing the mechanism and strength of streaming potential generation. When an external force (such as pressure gradient ∇p or evaporation-driven capillary flow) acts on the electrolyte solution, causing it to flow through microchannels such as porous membranes or capillaries, this directional flow drives the migration of charged particles within the diffusion layer of the double layer. For the steady-state, incompressible fluid flow potential ($E_{\text{streaming}}$), the Helmholtz–Smoluchowski equation can approximately describe in a simple capillary model:

$$E_{\text{streaming}} = \frac{\varepsilon\zeta}{\eta\lambda}\Delta p \quad (1)$$

where ε and η are the dielectric constant and viscosity of the fluid, ζ is the zeta potential, and λ is the conductivity of the solution. The migration of these charged particles results in charge accumulation in the downstream region of the solution, thereby establishing a potential difference between the upstream and downstream regions, which is defined as the flow potential. Simultaneously, the motion of the charged particles not only creates a potential difference but also generates a corresponding current, known as the flow current.[9]

In 2017, Zhou and co-workers[24] developed a porous carbon nanoparticle film generator device that harnessed the capillary phenomenon during water evaporation to drive the relative motion among carbon nanoparticles, thereby generating a flow potential within the carbon layer and achieving a voltage output as high as 1 V.

2.3 Parameter synergistic regulation mechanism

The core performance of MEG is synergistically governed by the material's pore structure (pore size, porosity) and environmental humidity gradients. Within the ion diffusion gradient mechanism, nanoscale channels enhance the local electric field through electric double layer overlap, thereby promoting ion migration, while high porosity provides continuous transport pathways that boost ionic conductivity.[26] The humidity gradient acts as the direct driving force, establishing an ion concentration difference that generates a diffusion current.[27] For the streaming potential mechanism, nanoscale pores not only intensify the electric double layer effect but also create stronger capillary forces to drive water flow. A high-porosity network ensures sufficient water channels and interfacial area.[28] Here, the humidity gradient serves as an indirect driver, sustaining directional water flow *via* evaporation to produce an electrical potential.[29] In practice, these two mechanisms often operate synergistically; for instance, highly porous materials under significant humidity gradients can simultaneously optimize both ion diffusion and streaming potential, collectively enhancing electrical energy output.

2.4 Other potential mechanisms

Electrochemical redox reactions can serve as an active regulation and performance enhancement strategy for MEG. Specific approaches include: utilizing metal oxidation reactions of active electrodes to provide an ion source, constructing surface functional group gradients to drive ion migration, or employing Schottky junctions to rectify current for stable DC output. For example, Yu *et al.*[30] designed a photosensitive MEG that uses photogenerated carriers to convert H^+ into H_2, thereby re-establishing the H^+ concentration gradient. Under 80% humidity, illumination increased the output voltage from 0.55 V to 0.65 V and the power density from 8.26 μW cm^{-2} to 26.7 μW cm^{-2}. In heterostructure systems, interfacial chemical potential differences can induce spontaneous ion migration and exchange. For instance, Wang and colleagues[16] reported a

Jianning Ding

Jianning Ding is a full professor at Yangzhou University and the head of Institute of Technology for Carbon Neutralization, China. He received his PhD degree from Tsinghua University. His research interests include the fundamentals of micro–nano device and system design and manufacturing, new energy materials, devices and equipment, and tribology.

Songnan Qu

Songnan Qu is a full professor at the Institute of Applied Physics and Materials Engineering (IAPME), University of Macau. He received B.S. and Eng.D. degrees from the Institute of Materials Science and Engineering at Jilin University. His research interests include energy storage and conversion, high-efficiency luminescence with controlled bandgap of carbon dots, solid-state light-emitting devices of carbon dots, and their applications of carbon nanodots in bioimaging and cancer diagnosis and treatment.

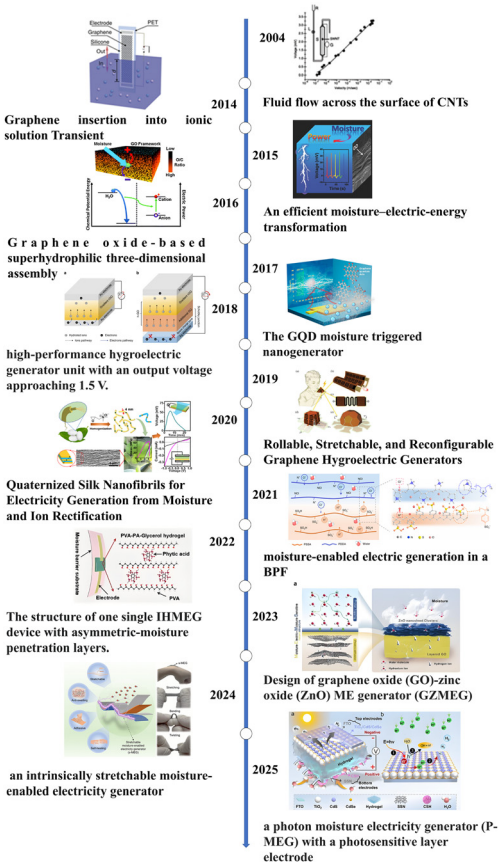

Fig. 1 Timeline showing the key developments in MEG.[8,11–22] Reproduced from ref. 21 with permission from The American Association for the Advancement of Science, copyright 2003. Reproduced from ref. 22 with permission from Springer Nature, copyright 2014. Reproduced from ref. 8 with permission from John Wiley and Sons, copyright 2015. Reproduced from ref. 11 with permission from Royal Society of Chemistry, copyright 2016. Reproduced from ref. 12 with permission from American Chemical Society, copyright 2017. Reproduced from ref. 13 with permission from Springer Nature, copyright 2018. Reproduced from ref. 14 with permission from John Wiley and Sons, copyright 2019. Reproduced from ref. 15 with permission from American Chemical Society, copyright 2020. Reproduced from ref. 16 with permission from Springer Nature, copyright 2021. Reproduced from ref. 17 with permission from John Wiley and Sons, copyright 2022. Reproduced from ref. 18 with permission from Springer Nature, copyright 2023. Reproduced from ref. 19 with permission from American Chemical Society, copyright 2024. Reproduced from ref. 20 with permission from John Wiley and Sons, copyright 2025.

PDDA/PSS heterojunction MEG, where bidirectional ion gradients enable ion exchange at the interface, achieving a high voltage of 1.38 V and a power density of 5.52 μW cm^{-2}. Additionally, interfacial capacitance effects (*e.g.*, Schottky contacts or capacitive electrodes) can enhance output stability by storing charge and rectifying ionic current. Sun *et al.*[31] constructed an MEG with symmetrically opposed charged electrodes and an electrolyte-loaded nanofiber membrane. The device remarkably sustained a stable output of 0.7 V and 3 μA for 120 hours and maintained high response sensitivity across

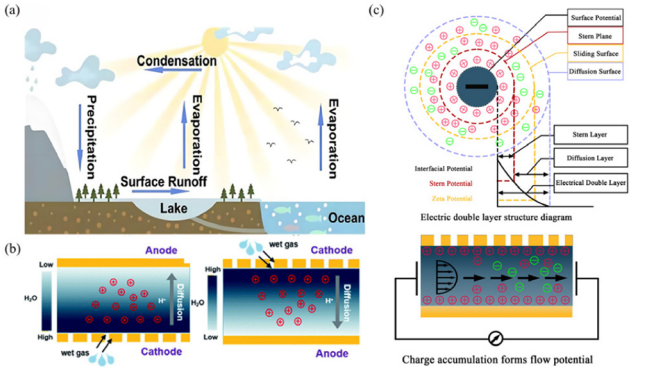

Fig. 2 (a) Illustration of abundant and sustainable moisture in the environment.[5] Reproduced from ref. 5 with permission from Elsevier, copyright 2022. (b) Schematic diagram of ion gradient diffusion mechanism.[25] Reproduced from ref. 25 with permission from Royal Society of Chemistry, copyright 2018. (c) Streaming potential mechanism diagram.

a broad humidity range (35–95%), which represents a significant advancement in current MEG technology.

3. MEG devices based on carbon materials

In MEG technology, the choice of hygroscopic layer material is crucial. Compared to easily degradable biomass materials,[32–34] polymers with poor stability,[35–38] and inorganic semiconductors with complex preparation processes,[39,40] carbon-based materials exhibit unique comprehensive advantages: their excellent intrinsic conductivity provides efficient pathways for electron transport; their surface-rich oxygen/nitrogen functional groups enable simultaneous water capture and proton dissociation; and their highly tunable multidimensional structures (from zero-dimensional quantum dots to three-dimensional porous networks) can precisely optimize water adsorption and ion transport paths.[41] Consequently, carbon-based materials have been widely used in MEG devices, and their performance is shown in Table 1 and Fig. 3.

3.1 Graphene quantum dots and carbon polymer dots

Carbon nanodot materials, due to their small nanoscale size and large specific surface area, exhibit unique advantages in MEG. Graphene quantum dots (GQDs) with typical diameters less than 10 nm are important representatives in this field. Huang *et al.*[12] reported a highly efficient moisture-triggered nanogenerator based on GQDs (Fig. 4f). The device utilized electrochemically polarized GQDs to create an oxygen group gradient. Leveraging the small size (2–5 nm), high specific surface area, and abundant oxygen-containing functional groups of GQDs, the device achieved 0.27 V voltage and 1.86 mW cm^{-2} power density under 70% relative humidity variation, demonstrating excellent current output capability. However, its power generation process relied on humidity cycling, resulting in intermittent pulsed output, making con-

Table 1 Summary and comparison of MEGs based on carbon materials

No.	Material	V_{oc}	I_{sc} or J_{sc}	Power	Cycle stability	RH	Ref.
1	GQD	0.27 V	27.7 mA cm^{-2}	1.86 mW cm^{-2}	150	70%	12
2	GCL	0.23 V	0.4 μA cm^{-2}	0.093 μW cm^{-2}	10	70%	44
3	3D-GO	0.26 V	3.2 mA cm^{-2}	~1 mW cm^{-2}	200	5%–80%	11
4	PGL	0.6 V	0.58 mA cm^{-2}	—	40	80%	45
5	GO/PVA	0.85 V	92.8 μA cm^{-2}	1.36 μW	—	75%	5
6	CNT/SA-hydrogel	1.03 V	23.8 μA cm^{-2}	9.12 μW cm^{-2}	30	60%	46
7	GO	0.48 V	7.23 μA cm^{-2}	0.41 μW	—	60%	47
8	GCF	1.10 V	56.2 μA cm^{-2}	61.8 μW cm^{-2}	—	90%	48
9	GO	0.45 V	0.9 μA cm^{-2}	2.02 μW cm^{-2}	—	85%	49
10	GO	0.7 V	12 mA cm^{-2}	—	100+	25%–85%	50
11	GO	0.35 V	5 μA cm^{-2}	0.42 μW cm^{-2}	—	—	8
12	GO/PAAS	0.6 V	1.2 μA cm^{-2}	0.07 mW cm^{-2}	100	80%	51
13	GO	0.04 V	0.3 mA cm^{-2}	—	1000	5%–35%	52
14	GO	0.3 V	0.7 μA cm^{-2}	0.21 μW cm^{-2}	—	70%	53
15	GO/copolymers	0.018 V	6.4 μA cm^{-2}	0.7 mW cm^{-2}	—	94%	54
16	PEDOT:PSS/GO	0.49 V	9.6 μA cm^{-2}	18.5 μW cm^{-2}	—	84%	55
17	GO film	0.18 V	1.1 μA	0.102 μW	100	15%–95%	14
18	h-GO	1.52 V	136 nA	32 mW cm^{-3}	50	10%–90%	13
19	CDs	0.04 V	142 nA	—	—	96%	25
20	SA/GO	0.7 V	2 mA	37 μW cm^{-2}	—	30%	56

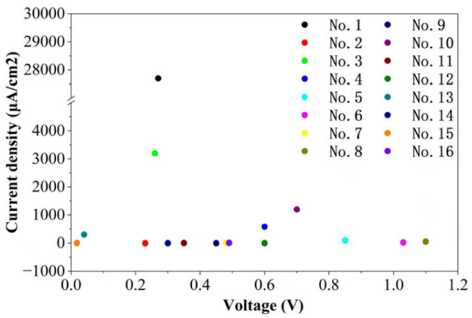

Fig. 3 Output voltage and current density of representative devices.[11,12,44,46–51,53,54,57–61]

tinuous power supply difficult. To enhance structural stability and practicality, Han *et al.*[42] embedded GQDs as "nano-charge sources" into graphene oxide fibers, constructing a fibrous osmotic energy generator with directed ion channels (Fig. 4c). The introduction of GQDs increased the surface charge density to 1.12 mC m^{-2} and improved ionic conductivity by approximately 5 times, achieving a power density of 0.25 W m^{-2} under a salinity gradient of 1000, showing its potential in continuous osmotic energy conversion. Nonetheless, this fiber structure still faced challenges such as high preparation complexity and insufficient mechanical flexibility and wearability. Addressing these challenges, Guo *et al.*[43] further compounded graphene dots with polystyrene sulfonate/polyvinyl alcohol (PSS/PVA) to develop a proton-conducting membrane with excellent mechanical strength (25.77 MPa) and self-healing ability (Fig. 4g). The introduction of graphene dots constructed fast proton transport channels, increasing the ionic conductivity to 1.41 S m^{-1}, and achieved continuous output of 0.31 V voltage and 23 μA current for 120 minutes under 83% humidity, significantly improving the bottleneck of low current output in traditional polyelectrolytes.

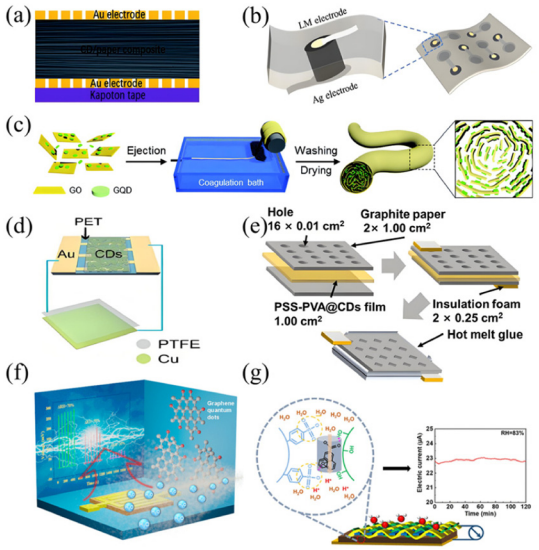

Fig. 4 (a) Cross-sectional diagram of CDs/paper device.[25] Reproduced from ref. 25 with permission from Royal Society of Chemistry, copyright 2018. (b) Preparation process of the MEG device based on PA-CPDs.[83] Reproduced from ref. 83 with permission from John Wiley and Sons, copyright 2023. (c) Schematics showing the wet-spinning process of the GQD-GO fiber.[42] Reproduced from ref. 42 with permission from Royal Society of Chemistry, copyright 2019. (d) Humidity sensors based on carbon nanodots.[84] Reproduced from ref. 84 with permission from Elsevier, copyright 2022. (e) Schematic illustration of the fabrication process for a MEG.[85] Reproduced from ref. 85 with permission from Elsevier, copyright 2023. (f) Working principle of the GQD moisture triggered nanogenerator.[12] Reproduced from ref. 12 with permission from American Chemical Society, copyright 2017. (g) Moisture electricity generation performance and hydrogen bond network structure of PPG–MEG.[43] Reproduced from ref. 43 with permission from American Chemical Society, copyright 2024.

Compared with graphene quantum dots, carbonized polymer dots (CPDs) possess a richer variety of surface groups, rendering them suitable for the fabrication of MEG devices.

The concept of CPDs was first proposed by Yang and co-workers at Jilin University, with its luminescent properties widely acknowledged in the field.[62–81] With ongoing research, the advantages of CPDs are continually being uncovered. CPDs not only retain the excellent properties of conventional power-generating materials but also exhibit organic molecular characteristics on their surfaces, offering notable benefits in designability, scalability, and versatility (Fig. 4b).[82] These advantageous features thus lay a solid foundation for constructing ideal power-generating materials.[83] In 2018, our team first applied CPDs to the field of MEG (Fig. 4a).[25] CPDs were printed on a paper substrate, and by constructing an asymmetric moisture absorption structure. A single device can continuously supply power for 100 minutes, with a maximum output voltage of 40 mV and a current of 142 nA. Leveraging its humidity-responsive characteristics, we explored applications in breath sensing and tactile sensing, showcasing excellent stability and repeatability. Building on these advancements, Shan and co-workers[84] synthesized CPDs using citric acid as a precursor and fabricated a humidity sensor (Fig. 4d). This device demonstrated high sensitivity and superior long-term stability and repeatability over a wide RH range. Subsequently, Hu and co-workers[85] selectively oxidatively etched coal tar pitch with a formic acid and hydrogen peroxide mixture to obtain a CPDs suspension (Fig. 4e), which was then incorporated into a PSS/PVA polyelectrolyte membrane, resulting in a highly efficient humid power generator with high sustained output voltage and short-circuit current density. Meanwhile, our team[83] developed an all-weather, efficient, and integrable CPDs-based MEG by regulating the surface groups of CPDs and designing a heterogeneous electrode structure. Under 85% ambient humidity, the device operates continuously and stably, delivering an output voltage as high as 0.8 V and a current density of 1.6 mA cm^{-2}, representing the highest current value and power density among all humid power generation devices to date.

3.2 Carbon nanotubes

Carbon nanotubes (CNTs), due to their one-dimensional hollow structure, excellent conductivity, and rapid capillary effect, are considered ideal hygroscopic layer materials in the field of MEG. Their surfaces, which can be modified with abundant functional groups, provide favourable conditions for water adsorption and proton transport. Xue *et al.*[24] in 2015 first proposed a device based on onion-like carbon black (CB) nanoparticles and multi-walled carbon nanotube (MWCNT) electrodes (Fig. 5b), utilizing capillary action to draw water up 2 cm through the CB layer, inducing a 1 V open-circuit voltage that remained stable for 8 days. However, this device had significant drawbacks: the output power was only 150 nA, and its performance was highly dependent on ambient temperature and humidity fluctuations (relative humidity > 70%), limiting its application in dynamic environments. Huang *et al.*[46] addressed these issues by embedding functionalized CNTs into a polybenzimidazole/polyvinyl alcohol (PSPC) heterogeneous gel (Fig. 5c). The CNT network served as a continuous

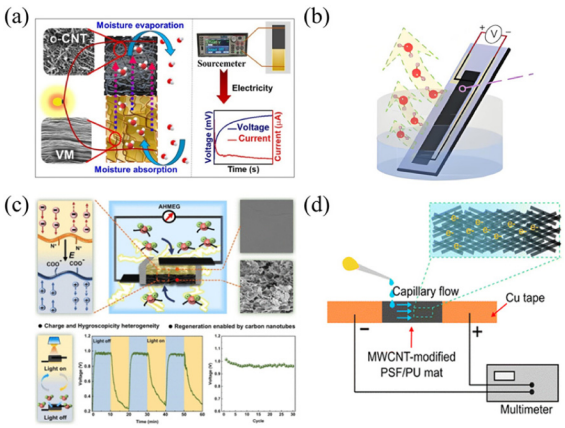

Fig. 5 (a) Schematic of working and output performance of MEG.[87] Reproduced from ref. 87 with permission from Elsevier, copyright 2024. (b) Schematic of device. The device consists of a CB sheet and two MWCNT electrodes on a quartz substrate.[24] Reproduced from ref. 24 with permission from Springer Nature, copyright 2017. (c) Biomimetic principles, structure and regeneration performance of PSPC-based AHMEGs.[46] Reproduced from ref. 46 with permission from American Chemical Society, copyright 2025. (d) Schematic illustration of the operation method of MPG.[86] Reproduced from ref. 86 with permission from Royal Society of Chemistry, copyright 2023.

conductive skeleton throughout the active layer, significantly enhancing charge transport efficiency. When moisture migrated between the porous SPC layer and the dense PAETA layer, the CNTs rapidly responded to interfacial potential changes, achieving a sustainable voltage output of 0.85 V. The device showed no performance degradation after 30 cycles, solving the stability issues of early devices, but the response speed was limited by the moisture absorption kinetics of the material, making it difficult to meet the real-time power supply needs of IoT sensors. Faramarzi *et al.*[86] further introduced a 0.6 M NaCl solution and used cation- and anion-modified MWCNTs to construct CNT films with alternating charge distribution (Fig. 5d). This precisely controlled layered stacking structure enhanced interfacial charge separation capability, and with the assistance of the salt solution, increased the V_{oc} to 1000 mV, the short-circuit current to 1.5 mA, and the power density by nearly an order of magnitude (12.5 μW cm^{-2}). This scheme significantly improved ion transport efficiency, but reliance on external liquid supply limited portability, and the need for periodic electrolyte replacement increased maintenance costs. In contrast, Saikia *et al.*[87] developed an oxidized CNT-vermiculite (o-CNT-VM) heterogeneous membrane that output voltages up to several hundred volts within a broad temperature range of 0–80 °C (Fig. 5a). Doping with LiCl increased the power density by 15 times (reaching 187.5 μW cm^{-2}), and it could directly power devices like calculators.

3.3 Graphene and its derivatives

GO, as a representative of the first-generation MEG materials, provides a key physicochemical foundation for water molecule adsorption and proton dissociation through its surface-rich

oxygen-containing functional groups and layered nanostructure.[88] From a materials chemistry perspective, the performance of GO is closely related to its defect degree and the control of oxygen functional groups. For example, carboxyl groups (–COOH), due to their lower pK_a values, are more easily ionized to release H^+ at ambient humidity, serving as the primary proton source; while hydroxyl groups (–OH) mainly promote the rapid transport of water molecules by forming hydrogen bond networks. DFT calculations can quantitatively compare the adsorption energy of water molecules on different functional groups like –COOH and C=O, and visualize their charge density difference, thereby revealing the strength and nature of water–solid interactions at the electronic level. The works by Qu and colleagues constitute a landmark achievement in the development of GO-based MEGs. In 2015, they developed an asymmetric functionalization strategy for GO films, creating a gradient distribution of oxygen-containing groups; by employing a moisture-induced electric field-assisted annealing (MEA) technique, they achieved an output voltage of 35 mV. This result provided key insights into how such asymmetry enhances ion gradient formation (Fig. 6a).[8] Subsequently, they fabricated a three-dimensional GO framework (G-3D-Go) using a combination of freeze-drying and compression molding techniques. The hierarchical porous structure of this framework improved water adsorption efficiency and maintained continuous ion transport pathways, resulting in an increased output voltage of 0.26 V (Fig. 6c).[11] Moreover, the integration of laser processing created a heterogeneous distribution of oxygen-containing functional groups. Coupled with Ag/GO–Au interfacial engineering, this approach elevated the output voltage of a single device to a record 1.5 V for the first time,[15] providing a significant reference for high-power MEG development. Composite modification represents another key strategy for performance enhancement. For instance, Cheng *et al.*[16] constructed GO/rGO heterojunctions *via* ultrasonic mixing, which significantly improved ionic conductivity and output performance (Fig. 6b). The resulting flexible device maintained over 90% voltage stability after 3000 bending cycles. Furthermore, defect engineering has opened new avenues. Zhu *et al.*[5] achieved the directional conversion of surface epoxy groups to carbonyl groups *via* HCl treatment (Fig. 6d), with the reaction path design benefiting from guidance by DFT calculations. The calculation results indicated that this conversion path significantly reduces the total energy of the system, suggesting its thermodynamic feasibility; meanwhile, the calculated reaction energy barriers provided references for optimizing the HCl treatment conditions. Guided by DFT calculations, the team successfully fabricated a device with record-breaking output performance and demonstrated excellent long-term stability (performance fluctuation < ±2% over 2 hours), setting a new benchmark for carbon-based MEG technology.

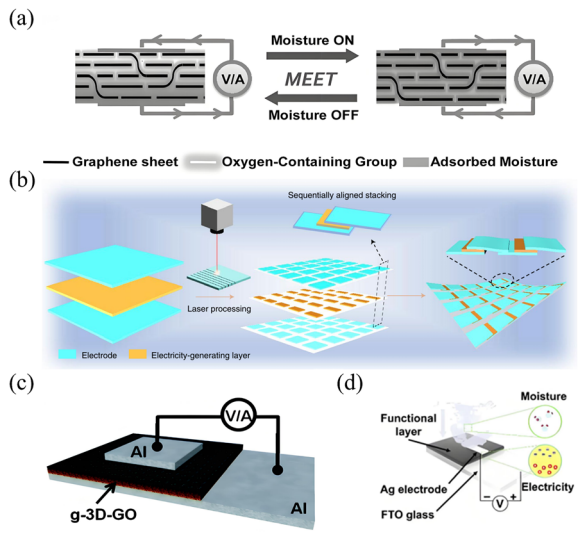

Fig. 6 (a) Schematic illustration of a MEET cycle.[8] Reproduced from ref. 8 with permission from John Wiley and Sons, copyright 2015. (b) Schematic illustration of large-scale integration of HMEG units by sequentially aligned stacking strategy.[16] Reproduced from r ef. 16 with permission from Springer Nature, copyright 2021. (c) Schematic illustration of a prototype CPEh based on g-3D-GO that is sandwiched by aluminium electrodes.[11] Reproduced from ref. 11 with permission from Royal Society of Chemistry, copyright 2016. (d) Structure illustration of MEG device.[5] Reproduced from ref. 5 with permission from Elsevier, copyright 2022.

3.4 Carbon black

In the field of moisture-induced power generation, constructing three-dimensional material systems with optimized pore structures and interfacial characteristics is a key pathway to achieving high-performance energy conversion. Such materials, leveraging their inherent high specific surface area and complex pore networks, can effectively facilitate the rapid adsorption, directional transport, and continuous evaporation of ambient moisture, thereby providing an ideal platform for establishing and maintaining stable ion concentration gradients. Among them, carbon black (CB), with its excellent conductivity, abundant surface functional groups, and tunable microstructure, has emerged as an ideal choice for constructing high-performance 3D moisture-enabled power generation materials, opening new avenues for developing low-cost, high-efficiency moisture energy harvesting technology. Wen *et al.*[89] reported a moisture-induced generator (SHMEG) based on a self-gradient hydrogel (Fig. 7a). This device was fabricated by inducing the directional diffusion of a polyacrylamide/glycerol/sodium chloride pre-gel solution on a knitted fabric loaded with carbon black, successfully establishing significant concentration gradients of ions and water molecules. The device maintained voltage outputs of 0.5 V and 0.7 V in low humidity (20%) and low-temperature (−10 °C) environments, respectively, demonstrating exceptional environmental adaptability. Furthermore, its 300% tensile strain revealed potential for applications in wearable strain sensing. However, performance degradation occurred after multiple charge/discharge cycles, primarily attributed to the weakening of the ion concentration gradient caused by sodium ion diffusion. Although the corrosion of silver electrodes contributed to the voltage output, it

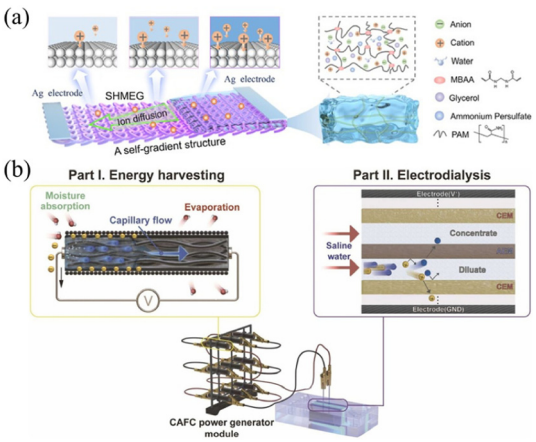

Fig. 7 (a) Schematic illustration of the preparation and structure of SHMEG.[89] Reproduced from ref. 89 with permission from John Wiley and Sons, copyright 2025. (b) Schematic of a hybrid ED system coupled with stacked cellulose acetate fiber columns (CAFC) power generators.[90] Reproduced from ref. 90 with permission from Elsevier, copyright 2024.

might compromise the long-term stability of the device. In contrast, Lee *et al.*[90] proposed a more cost-effective technical approach (Fig. 7b). They used commercial cigarette filter rods composed of cellulose acetate fibers as substrates and utilized capillary forces to drive the coating of carbon black particles, constructing a moisture-enabled generator based on the streaming potential effect within nanochannels. By optimizing the carbon black loading concentration to 6.25 g mL^{-1} and employing a customized module to serially integrate 90 units, they achieved high voltage outputs ranging from 13.5 V to 22 V. The notable advantages of this design include the low cost of raw materials, the simplicity of the fabrication process, and the environmental benefits of recycling waste filters. However, the power generation performance was significantly influenced by ambient humidity fluctuations, and used filters exhibited a decline in performance (voltage output dropping to approximately 0.195 V) due to the adsorption of surface contaminants.

4. Key performance of MEG

Besides power generation capability, factors such as scalability, flexibility, stability, operational lifetime, and integration compatibility determine the application prospects and future potential of MEG devices.

4.1 Scalability and flexible

MEG devices often use flexible substrates (*e.g.*, PET, cotton fabric, paper) as supporting materials. These materials not only provide good mechanical properties but their porous or hydrophilic characteristics also help capture and transport moisture. For example, the cellulose network in paper substrates can form natural capillary water channels, significantly improving moisture response speed. However, the trade-off between the mechanical strength and environmental durability of existing flexible substrates remains a problem to be solved.

4.2 Stability and operational lifetime

The long-term stability of MEG devices is a key consideration for their practical application. Studies have shown that some carbon-based MEG devices can maintain good electrical output performance even after hundreds of hours of continuous operation or thousands of humidity cycles. For instance, some graphene GO-based devices show less than 10% voltage output attenuation after 1000 cycles, demonstrating good cycle stability. However, the actual lifespan of devices is still constrained by various factors such as material degradation, electrode corrosion, and contaminant clogging, particularly in high humidity, high temperature, or polluted environments where performance degradation is more pronounced, severely limiting their long-term application in outdoor environments.

4.3 Influence of environmental temperature and humidity

The output performance of MEG is highly dependent on environmental relative humidity (RH) and temperature. Most devices perform best in the RH range of 60%–90%, while output decreases significantly in low humidity (<30%) or supersaturated (>95%) environments. Temperature changes indirectly regulate power generation efficiency by affecting water adsorption rate and ion migration speed. Although introducing hygroscopic salts or constructing porous hydrogel structures can improve device adaptability in dry or low-temperature environments to some extent, the environmental robustness of current MEG devices is still insufficient to cope with complex and variable practical application scenarios.

4.4 Large-scale integration

Achieving large-scale integration of MEG devices is a key step in promoting their transition from the laboratory to practical applications. Currently, the combination of flexible substrates (*e.g.*, PET, textiles, paper) and printable electronics technology provides a feasible path for the scaled manufacturing of MEG. Through screen printing, inkjet printing processes, MEG units with consistency can be efficiently prepared on flexible substrates, and modular series or parallel integration can be achieved to enhance the system's total output voltage or current. However, large-scale integration of MEG still faces many challenges: firstly, the consistency and stability of unit performance are difficult to maintain on a macroscopic scale, especially prone to output imbalance in complex humidity fields; secondly, issues such as interfacial contact resistance during integration, packaging reliability, and the durability of flexible connecting lines directly affect the overall efficiency and lifespan of the integrated system; furthermore, the structural design of integrated devices needs to balance humidity response speed, mechanical flexibility, and environmental adaptability, placing higher demands on materials and processes.

5. Application of the MEG

MEG is an emerging energy conversion technology that continuously harvests ambient water vapor and converts it into electrical energy. Its integratable and miniaturizable characteristics endow it with immense application potential in future distributed energy systems.[91]

5.1 Power source

In recent years, optimization of materials and structural design has increased the open-circuit voltage of individual MEG units from tens of microvolts (μV) to the volt (V) level, and the current density from tens of nA cm^{-2} to hundreds of μA cm^{-2}. Furthermore, through effective device integration strategies, MEG systems are now capable of providing stable and continuous power output for electronic devices (Fig. 8a–c).[92–96] For example, Qu and co-workers[16] developed a heterogeneous film MEG that successfully outputs kilovolt-range voltages through device integration. Tao and co-workers[97] created a MEG based on ultrahigh molecular hydrogel that not only produces a power density as high as 0.11 mW cm^{-2} but also achieves an output of 65 mA of electrical current when integrated.

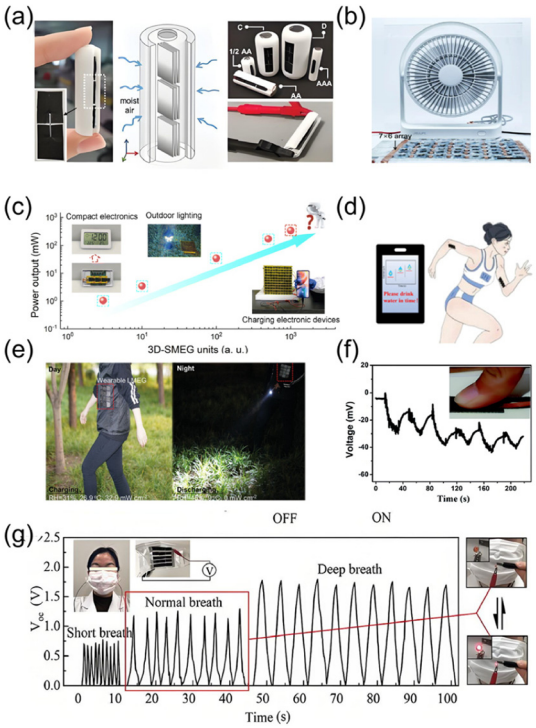

Fig. 8 (a) Multiple AHS units are connected by staples and embedded in a 3D-printed battery case.[92] Reproduced from ref. 92 with permission from John Wiley and Sons, copyright 2022. (b) A commercially available electric fan powered by a 7 × 6 i-eMEH array.[93] Reproduced from ref. 93 with permission from Springer Nature, copyright 2025. (c) Integrate the 3D-SMEG system to drive commercial appliances.[94] Reproduced from ref. 94 with permission from Royal Society of Chemistry, copyright 2025. (d) SP-HEG as a self-powered and wearable sweat monito-ring platform.[98] Reproduced from ref. 98 with permission from John Wiley and Sons, copyright 2022. (e) Left: LMEGs are integrated with garment and charged a capacitor during the day. Right: the electricity stored in the capacitor could light up a flashlight at night.[108] Reproduced from ref. 108 with permission from John Wiley and Sons, copyright 2025. (f) Measured voltage of the CDs/paper device when the finger was pressed and released periodically.[25] Reproduced from ref. 25 with permission from Royal Society of Chemistry, copyright 2018. (g) The digital photos of the LED powered by the 5BMIEGs-9 under normal breath in a dim room.[104] Reproduced from ref. 104 with permission from John Wiley and Sons, copyright 2021.

5.2 Sensors

In addition to serving as a power source, the MEG itself exhibits a highly sensitive response to ambient humidity, demonstrating significant potential in sensor applications. As a sensor, the generator device can function as a sensing unit. For example, it can serve as a human motion sensor (Fig. 8d),[98–101] a touch sensor (Fig. 8f),[25,102,103] or a respiration sensor (Fig. 8g).[104–107] When used as a respiratory analyser, the current and voltage variations induced by moisture can help distinguish between normal and rapid breathing. MEG can also be integrated into touch sensors; as a finger approaches a touchscreen, the moisture generator absorbs water from the fingertip, and changes in LED brightness provide feedback regarding the finger's position.

Currently, most of these applications are still in the early experimental phase (Table 2), but they have already demonstrated potential in several promising areas. To evaluate the actual development stage of MEG technology, this article adopts a simplified framework based on the NASA technology readiness level model for evaluation. This framework defines TRL 1–3 as the "basic research and principle verification phase", TRL 4–6 as the "laboratory prototype development and optimization phase", and TRL 7–9 as the "system testing and near commercialization phase". Table 2 presents the current development stage, typical demonstrations, challenges, and corresponding technical readiness levels of MEG technology under different application directions based on this standard. With the continued enhancement of MEG output characteristics, future innovations will focus on optimizing advanced materials to extend its applications across different fields.

6. Summary and outlook

Amid the growing global demand for sustainable energy, various nanogenerator technologies have developed rapidly, among which triboelectric generators (TENG), piezoelectric generators (PZG), pyroelectric generators (PYG), and MEG have achieved notable progress in recent years. These power generation methods possess distinct characteristics: TENG devices utilize low-cost materials, are easy to integrate, and can be fabricated into flexible devices, but TENG output is unstable, charges dissipate easily under high humidity, and long-term use can cause material wear (Fig. 9d).[111–113] PZG feature fast response times and compact structures, facilitating easy embedding, but their output is characterized by high voltage

Table 2 Technology readiness level

Application field	Material type	TRL	Example demonstration	Challenges	Ref
Environmental adaptive power generation	Polyelectrolyte film, GO	4–6 (laboratory stage)	Multiple power generation units integrated to provide power for commercial electronic technology.	Low power density and poor working stability	11, 16 and 47
Self-powered wearable electronic devices	GO, carbon nanotubes	4–6 (laboratory stage)	Provide power to electronic devices and monitor vital signs of the human body.	High cost, low mechanical strength	45, 58, 86, 109 and 110
Environmental monitoring and sensor connection	Hydrogel	4–6 (laboratory stage)	Monitor humidity, weather, and lighting.	Energy supply stability and environmental adaptability need to be improved	20
Large scale and distributed power generation	Polyelectrolyte film	1–3 (principle verification stage)	Integrating multiple power generation units to drive loads indicates the feasibility of the principle of integrated amplification.	Low energy density, there is still a big gap from practical application	16

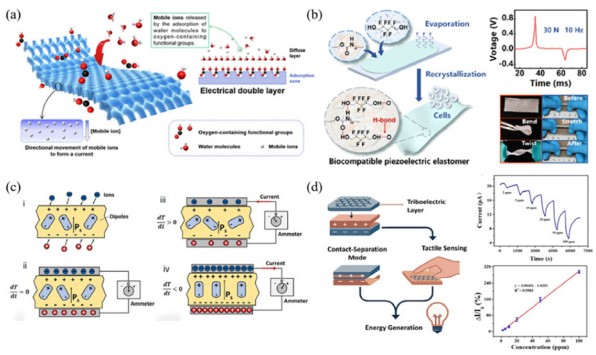

Fig. 9 (a) Moisture-enabled electric generator.[122] Reproduced from ref. 122 with permission from American Chemical Society, copyright 2024. (b) Piezoelectric generator.[117] Reproduced from ref. 117 with permission from American Chemical Society, copyright 2025. (c) Pyroelectric generator.[118] Reproduced from ref. 118 with permission from Elsevier, copyright 2023. (d) Triboelectric nanogenerators.[111] Reproduced from ref. 111 with permission from John Wiley and Sons, copyright 2025.

and low current, requiring appropriate power management circuits. Commonly used lead-based piezoelectric materials suffer from poor flexibility, brittleness under impact, and certain toxicity (Fig. 9b).[114–117] PYG exhibit high temperature sensitivity and can efficiently harvest waste heat from the environment, such as body heat or industrial process heat, thereby improving energy utilization efficiency. Using $BaTiO_3$ enables operation from −50 °C to 100 °C, while $LiTaO_3$ can function from −200 °C to 500 °C, covering most scenarios. However, PYG requires a dynamic heat source, and ceramics with high pyroelectric coefficients (*e.g.*, lead zirconate titanate) involve complex processing and yield low output power (Fig. 9c).[118–121] In contrast, MEG offers a pollution-free generation process, utilizes ubiquitous resources (atmospheric moisture), can generate electricity stably and continuously in most environments, often employs flexible materials, and, as the materials are generally biocompatible, can be developed into wearable devices. MEGs fabricated from biomass materials are not only low-cost but also biodegradable. They are easily integrable to significantly enhance total output power, and require no maintenance, reducing costs. Consequently, MEG holds significant advantages among the various nanogenerator technologies (Fig. 9a).[122]

However, current MEG technology still faces several significant challenges that need to be addressed:

(1) The primary issue lies in its inadequate output capacity, manifested as a power density significantly lower than other emerging energy harvesting technologies such as TENG, PZG, and PYG. The power output of MEG is generally confined to the microwatt level, whereas TENG can achieve instantaneous power in the watt range, and the power density of photovoltaic devices is several orders of magnitude higher. This extremely low power density renders MEG incapable of independently powering most microelectronic devices, thereby constraining its practical applications.

(2) Another limitation is reflected in the singularity of its energy source and its heavy reliance on specific environmental conditions. MEG's energy harvesting is entirely dependent on ambient humidity, making it far less flexible than TENG, which can harvest energy from diverse mechanical sources like wind, rain, and human motion, or pyroelectric generators that can utilize various forms of waste heat. This strong dependence on a single environmental factor severely restricts the application scope of MEG.

(3) The energy conversion process in MEG is passive and slow, relying on the adsorption, diffusion, or evaporation of water molecules—a physicochemical process that cannot effectively respond to transient or high-frequency mechanical stimuli. In contrast, TENG and PZG can rapidly respond to mechanical excitation, giving them distinct advantages in harvesting energy from human activities and machine vibrations.

(4) Environmental adaptability and stability also pose serious challenges for MEG. Environmental contaminants (*e.g.*, dust, salts) can easily clog the material's nanochannels, leading to performance degradation. Its power generation performance also significantly decreases under humidity saturation conditions. In comparison, PYG can operate reliably for extended periods under stable temperature differences, and the environmental stability of photovoltaic technology has already been secured through mature encapsulation solutions.

(5) The large-scale integration of MEG devices remains a significant hurdle. Existing integration methods typically involve two separate steps: material synthesis and device integration. The process is complex, and the resulting integrated devices often suffer from poor integrity, flexibility, and consistency, hindering their scalable application.

Overall, research on humidity power generation is still in its early stages, yet its future development potential is immense. With further advancements in research, it is expected that the conversion efficiency and output power density of humidity power generation devices will significantly improve, enabling efficient, stable, and continuous power output, and making a valuable contribution to addressing energy shortages and excessive carbon dioxide emissions.

Author contributions

J. Tan: supervision, writing – original draft, funding acquisition; C. Tian: writing – original draft, visualization; L. Liu: investigation, writing – original draft; Y. Liu: visualization, writing – review & editing; J. Tan: supervision, writing – review & editing; Q. Li: conceptualization, funding acquisition, writing – review & editing; J. Ding: conceptualization, funding acquisition; S. Qu: conceptualization, supervision, writing – review & editing.

Conflicts of interest

The authors declare no conflict of interest.

Data availability

No primary research results, software or code have been included and no new data were generated or analysed as part of this review.

Acknowledgements

The authors acknowledge the support from the National Natural Science Foundation of China (No. 52473281 and 52572265), and the Natural Science Foundation of Jiangsu (BK20231537). This work was financially supported by the Science and Technology Development Fund of Macau SAR (0139/2022/A3, 0002/2024/TFP) and the University of Macau – Dr Stanley Ho Medical Development Foundation "Set Sail for New Horizons, Create the Future" Grant 2025 (SHMDF-OIRFS/2025/001).

References

1 G. Zhou, H. Xu, H. Song, J. Yi, X. Wang, Z. Chen and X. Zhu, *ACS Catal.*, 2024, **14**, 8694–8719.
2 M. J. Albert, *Alternatives: Global, Local, Political*, 2021, **46**, 89–98.
3 X. Wang, F. Lin, X. Wang, S. Fang, J. Tan, W. Chu, R. Rong, J. Yin, Z. Zhang, Y. Liu and W. Guo, *Chem. Soc. Rev.*, 2022, **51**, 4902–4927.
4 B. Shao, Y. Song, Z. Song, Y. Wang, Y. Wang, R. Liu and B. Sun, *Adv. Energy Mater.*, 2023, **13**, 2204091.
5 R. Zhu, Y. Zhu, F. Chen, R. Patterson, Y. Zhou, T. Wan, L. Hu, T. Wu, R. Joshi, M. Li, C. Cazorla, Y. Lu, Z. Han and D. Chu, *Nano Energy*, 2022, **94**, 106942.
6 D. Shen, W. W. Duley, P. Peng, M. Xiao, J. Feng, L. Liu, G. Zou and Y. N. Zhou, *Adv. Mater.*, 2020, **32**, 2003722.
7 F. Galembeck and T. A. L. Burgo, *Chemical Electrostatics, New Ideas on Electrostatic Charging: Mechanisms and Consequences*, Springer International Publishing, Cham, Switzerland, 2017.
8 F. Zhao, H. Cheng, Z. Zhang, L. Jiang and L. Qu, *Adv. Mater.*, 2015, **27**, 4351–4357.
9 W. Lu, W. L. Ong and G. W. Ho, *J. Mater. Chem. A*, 2023, **11**, 12456–12481.
10 Z. Zhang, X. Li, J. Yin, Y. Xu, W. Fei, M. Xue, Q. Wang, J. Zhou and W. Guo, *Nat. Nanotechnol.*, 2018, **13**, 1109–1119.
11 F. Zhao, Y. Liang, H. Cheng, L. Jiang and L. Qu, *Energy Environ. Sci.*, 2016, **9**, 912–916.
12 Y. Huang, H. Cheng, G. Shi and L. Qu, *ACS Appl. Mater. Interfaces*, 2017, **9**, 38170–38175.
13 Y. Huang, H. Cheng, C. Yang, P. Zhang, Q. Liao, H. Yao, G. Shi and L. Qu, *Nat. Commun.*, 2018, **9**, 4166.
14 C. Yang, Y. Huang, H. Cheng, L. Jiang and L. Qu, *Adv. Mater.*, 2019, **31**, 1805705.
15 W. Yang, L. Lv, X. Li, X. Han, M. Li and C. Li, *ACS Nano*, 2020, **14**, 10600–10607.
16 H. Wang, Y. Sun, T. He, Y. Huang, H. Cheng, C. Li, D. Xie, P. Yang, Y. Zhang and L. Qu, *Nat. Nanotechnol.*, 2021, **16**, 811–819.
17 S. Yang, X. Tao, W. Chen, J. Mao, H. Luo, S. Lin, L. Zhang and J. Hao, *Adv. Mater.*, 2022, **34**, 2200693.
18 Y. n. Yang, J. Wang, Z. Wang, C. Shao, Y. Han, Y. Wang, X. Liu, X. Sun, L. Wang, Y. Li, Q. Guo, W. Wu, N. Chen and L. Qu, *Nano-Micro Lett.*, 2023, **16**, 56.
19 W. He, P. Li, H. Wang, Y. Hu, B. Lu, C. Weng, H. Cheng and L. Qu, *ACS Nano*, 2024, **18**, 12096–12104.
20 F. Yu, Y. Zhang, L. Wang, X. Yang, Y. Yang, X. Li, Y. Gao, X. Zhang, W. Lü, K. Jiang, X. Sun and D. Li, *Adv. Mater.*, 2025, e09043.
21 S. Ghosh, A. K. Sood and N. Kumar, *Science*, 2003, **299**, 1042–1044.
22 J. Yin, Z. Zhang, X. Li, J. Yu, J. Zhou, Y. Chen and W. Guo, *Nat. Commun.*, 2014, **5**, 3582.
23 Z. Sun, X. Wen, L. Wang, D. Ji, X. Qin, J. Yu and S. Ramakrishna, *eScience*, 2022, **2**, 32–46.
24 G. Xue, Y. Xu, T. Ding, J. Li, J. Yin, W. Fei, Y. Cao, J. Yu, L. Yuan, L. Gong, J. Chen, S. Deng, J. Zhou and W. Guo, *Nat. Nanotechnol.*, 2017, **12**, 317–321.

25 Q. Li, M. Zhou, Q. Yang, M. Yang, Q. Wu, Z. Zhang and J. Yu, *J. Mater. Chem. A*, 2018, **6**, 10639–10643.
26 Y. Liang, F. Zhao, Z. Cheng, Q. Zhou, H. Shao, L. Jiang and L. Qu, *Nano Energy*, 2017, **32**, 329–335.
27 X. Liu, H. Gao, J. E. Ward, X. Liu, B. Yin, T. Fu, J. Chen, D. R. Lovley and J. Yao, *Nature*, 2020, **578**, 550–554.
28 Q. Lyu, B. Peng, Z. Xie, S. Du, L. Zhang and J. Zhu, *ACS Appl. Mater. Interfaces*, 2020, **12**, 57373–57381.
29 T. Chen, D. Zhang, X. Tian, S. Qiang, C. Sun, L. Dai, M. Zhang, Y. Ni and X. Jiang, *Carbohydr. Polym.*, 2022, **294**, 119809.
30 F. Yu, Y. Zhang, L. Wang, X. Yang, Y. Yang, X. Li, Y. Gao, X. Zhang, W. Lü, K. Jiang, X. Sun and D. Li, *Adv. Mater.*, 2025, **38**, e09043.
31 Z. Sun, X. Wen, L. Wang, J. Yu and X. Qin, *Energy Environ. Sci.*, 2022, **15**, 4584–4591.
32 L. Huang, Y. Tang, W. Liu, Q. Hu and X. Wei, *Carbohydr. Polym.*, 2024, **326**, 121649.
33 H. Zhong, S. Wang, Z. Wang and J. Jiang, *Chem. Eng. J.*, 2024, **486**, 150203.
34 H. He, J. Zhang, J. Pan, Z. Wang, M. Deng, X. Liu and F. Fu, *ACS Appl. Energy Mater.*, 2024, **7**, 2980–2988.
35 H. Zhang, N. He, B. Wang, B. Ding, B. Jiang, D. Tang and L. Li, *Adv. Mater.*, 2023, **35**, 2300398.
36 W. He, H. Wang, Y. Huang, T. He, F. Chi, H. Cheng, D. Liu, L. Dai and L. Qu, *Nano Energy*, 2022, **95**, 107017.
37 L. Wang, H. Wang, C. Wu, J. Bai, T. He, Y. Li, H. Cheng and L. Qu, *Nat. Commun.*, 2024, **15**, 4929.
38 W. Duan, B. Shao, Z. Wang, K. Ni, S. Liu, X. Yuan, Y. Wang, B. Sun, X. Zhang and R. Liu, *Energy Environ. Sci.*, 2024, **17**, 3788–3796.
39 Y.-M. Cao, Y. Su, M. Zheng, P. Luo, Y.-B. Xue, B.-B. Han, M. Zheng, Z. Wang, L.-S. Liao and M.-P. Zhuo, *ACS Nano*, 2023, **18**, 492–505.
40 D. Shen, M. Xiao, G. Zou, L. Liu, W. W. Duley and Y. N. Zhou, *Adv. Mater.*, 2018, **30**, 1705925.
41 W. Duan, Z. Sun, X. Jiang, S. Tang and X. Wang, *Nano Energy*, 2025, **134**, 110516.
42 K. H. Lee, H. Park, W. Eom, D. J. Kang, S. H. Noh and T. H. Han, *J. Mater. Chem. A*, 2019, **7**, 23727–23732.
43 L. Guo, Y.-B. Liu, W.-X. Li, J.-Y. Gong, W. Zuo, Y.-L. Liu and P. Fu, *ACS Appl. Nano Mater.*, 2024, **7**, 20913–20919.
44 S. Lee, H. Jang, H. Lee, D. Yoon and S. Jeon, *ACS Appl. Mater. Interfaces*, 2019, **11**, 26970–26975.
45 W. Ying, Z. Huang, Z. Liu, J. Liu, N. Pan, A. Jazzar, J. Zhang, H. Zhang, X. He, R. Wang and J. Wang, *Energy Environ. Sci.*, 2025, **18**, 9457–9467.
46 Z. Huang, T. Zhang, H. Cao, Z. Xu, A. Ju and Y. Zhao, *ACS Appl. Mater. Interfaces*, 2025, **17**, 7916–7928.
47 H. Liu, Y. Han, X. Zhang, Y. Zhang, G. Li, Z. Lin, Y. Lei, D. Chen and L. Xue, *J. Bionic Eng.*, 2025, **22**, 783–792.
48 J. Eun and S. Jeon, *ACS Appl. Mater. Interfaces*, 2022, **14**, 45289–45295.
49 H. Cheng, Y. Huang, F. Zhao, C. Yang, P. Zhang, L. Jiang, G. Shi and L. Qu, *Energy Environ. Sci.*, 2018, **11**, 2839–2845.
50 H. Cheng, Y. Huang, L. Qu, Q. Cheng, G. Shi and L. Jiang, *Nano Energy*, 2018, **45**, 37–43.
51 Y. Huang, H. Cheng, C. Yang, H. Yao, C. Li and L. Qu, *Energy Environ. Sci.*, 2019, **12**, 1848–1856.
52 F. Zhao, L. Wang, Y. Zhao, L. Qu and L. Dai, *Adv. Mater.*, 2017, **29**, 1604972.
53 C. Shao, J. Gao, T. Xu, B. Ji, Y. Xiao, C. Gao, Y. Zhao and L. Qu, *Nano Energy*, 2018, **53**, 698–705.
54 S. Daripa, K. Khawas, R. P. Behere, R. Verma and B. K. Kuila, *ACS Omega*, 2021, **6**, 7257–7265.
55 X. Qi, T. Miao, C. Chi, G. Zhang, C. Zhang, Y. Du, M. An, W.-G. Ma and X. Zhang, *Nano Energy*, 2020, **77**, 105096.
56 H. Li, Z. Ma, Z. Xu, Y. Wei, W. Tang, P. Li, Q. Huang, Q. Zou, H. Wang, M. Zhong and Z. Zhang, *Energy Technol.*, 2025, 2500236.
57 W. Ying, Z. Huang, Z. Liu, J. Liu, N. Pan, A. Jazzar, J. Zhang, H. Zhang, X. He, R. Wang and J. Wang, *Energy Environ. Sci.*, 2025, **18**, 9457–9467.
58 R. Zhu, Y. Zhu, F. Chen, R. Patterson, Y. Zhou, T. Wan, L. Hu, T. Wu, R. Joshi, M. Li, C. Cazorla, Y. Lu, Z. Han and D. Chu, *Nano Energy*, 2022, **94**, 106942.
59 F. Zhao, H. Cheng, Z. Zhang, L. Jiang and L. Qu, *Adv. Mater.*, 2015, **27**, 4351–4357.
60 F. Zhao, L. Wang, Y. Zhao, L. Qu and L. Dai, *Adv. Mater.*, 2017, **29**, 1604972.
61 X. Qi, T. Miao, C. Chi, G. Zhang, C. Zhang, Y. Du, M. An, W.-G. Ma and X. Zhang, *Nano Energy*, 2020, **77**, 105096.
62 Q. Li, H. Zhao, D. Yang, S. Meng, H. Gu, C. Xiao, Y. Li, D. Cheng, S. Qu, H. Zeng, X. Zhu, J. Tan and J. Ding, *Nano Lett.*, 2024, **24**, 3028–3035.
63 Q. Li, Z. Zhao, S. Meng, Y. Li, Y. Zhao, B. Zhang, Z. Tang, J. Tan and S. Qu, *SmartMat*, 2022, **3**, 260–268.
64 Q. Li, S. Meng, Y. Li, D. Cheng, H. Gu, Z. Zhao, Z. Tang, J. Tan and S. Qu, *Carbon*, 2022, **195**, 191–198.
65 S. Tao, S. Lu, Y. Geng, S. Zhu, S. A. T. Redfern, Y. Song, T. Feng, W. Xu and B. Yang, *Angew. Chem., Int. Ed.*, 2018, **57**, 2393–2398.
66 C. Kang, S. Tao, F. Yang, C. Zheng, Z. Qu and B. Yang, *Angew. Chem., Int. Ed.*, 2024, **63**, e202316527.
67 Y. Zhang, S. Ding, J. Yu, L. Sui, H. Song, Y. Hu, G. I. N. Waterhouse, Z. Tang and S. Lu, *Matter*, 2024, **7**, 3518–3536.
68 L. Tang, L. Ai, Z. Song, L. Sui, J. Yu, X. Yang, H. Song, B. Zhang, Y. Hu, Y. Zhang, Y. Tian and S. Lu, *Adv. Funct. Mater.*, 2023, **33**, 2303363.
69 J. Xue, X. Mao, X. Zhao, T. Xie, H. Hu, Z. Li and W. Gao, *J. Lumin.*, 2024, **275**, 120757.
70 J. Hu, M. Lei, L. Yan, L. Chen, Y. Yang, J. Zheng, X. Liu and B. Xu, *Chem. Eng. J.*, 2024, **489**, 151245.
71 M. Lei, J. Zheng, Y. Yang, L. Yan, X. Liu and B. Xu, *iScience*, 2022, **25**, 104884.
72 K. Jiang, X. Gao, X. Feng, Y. Wang, Z. Li and H. Lin, *Angew. Chem., Int. Ed.*, 2020, **59**, 1263–1269.

73 Y. Song, S. Zhu, S. Zhang, Y. Fu, L. Wang, X. Zhao and B. Yang, *J. Mater. Chem. C*, 2015, **3**, 5976–5984.
74 Y. Liu, D. Cheng, B. Wang, J. Yang, Y. Hao, J. Tan, Q. Li and S. Qu, *Adv. Mater.*, 2024, **36**, 2403775.
75 Y. Ding, X. Wang, M. Tang and H. Qiu, *Adv. Sci.*, 2022, **9**, 2103833.
76 Y. Shi, Y. Zhang, Z. Wang, T. Yuan, T. Meng, Y. Li, X. Li, F. Yuan, Z. a. Tan and L. Fan, *Nat. Commun.*, 2024, **15**, 3043.
77 Y. Liu, B. Wang, Y. Zhang, J. Guo, X. Wu, D. Ouyang, S. Chen, Y. Chen, S. Wang, G. Xing, Z. Tang and S. Qu, *Adv. Funct. Mater.*, 2024, **34**, 2401353.
78 C.-L. Shen, J.-H. Zang, Q. Lou, G.-S. Zheng, M.-Y. Wu, Y.-L. Ye, J.-Y. Zhu, K.-K. Liu, L. Dong and C.-X. Shan, *Appl. Surf. Sci.*, 2021, **559**, 149947.
79 Z. Zhou, P. Tian, X. Liu, S. Mei, D. Zhou, D. Li, P. Jing, W. Zhang, R. Guo, S. Qu and A. L. Rogach, *Adv. Sci.*, 2018, **5**, 1800369.
80 L. E. da Silva, O. L. d. L. Calado, S. F. de Oliveira Silva, K. R. M. da Silva, J. Henrique Almeida, M. de Oliveira Silva, R. d. S. Viana, J. N. de Souza Ferro, J. de Almeida Xavier and C. D. A. E. S. Barbosa, *J. Colloid Interface Sci.*, 2023, **651**, 678–685.
81 S. Hu, A. Trinchi, P. Atkin and I. Cole, *Angew. Chem., Int. Ed.*, 2015, **54**, 2970–2974.
82 C. Xia, S. Zhu, T. Feng, M. Yang and B. Yang, *Adv. Sci.*, 2019, **6**, 1901316.
83 Q. Li, Y. Qin, D. Cheng, M. Cheng, H. Zhao, L. Li, S. Qu, J. Tan and J. Ding, *Adv. Funct. Mater.*, 2023, **33**, 2211013.
84 J. Qin, X. Yang, C. Shen, Y. Chang, Y. Deng, Z. Zhang, H. Liu, C. Lv, Y. Li, C. Zhang, L. Dong and C. Shan, *Nano Energy*, 2022, **101**, 107549.
85 Z. Yan, N. Li, Q. Chang, C. Xue, J. Yang and S. Hu, *Chem. Eng. J.*, 2023, **467**, 143443.
86 P. Faramarzi, B. Kim, J. B. You and S.-H. Jeong, *J. Mater. Chem. C*, 2023, **11**, 2206–2216.
87 B. Saikia, M. Dey, P. Garg, R. Gogoi, R. Manik and K. Raidongia, *Chem. Eng. J.*, 2024, **497**, 154840.
88 S. Pramanik, C. Sengupta, S. Sharma, S. Mondal, D. K. Goswami and T. Mondal, *ACS Appl. Electron. Mater.*, 2024, **6**, 8689–8702.
89 X. Wen, Z. Sun, Y. Cho, M. S. Kim, K. Qin, Q. Zhou, C. Zhang, L. Wang, I. D. Kim and X. Qin, *Adv. Funct. Mater.*, 2025, **35**, e06700.
90 S.-H. Lee, J.-Y. Kim, J. Kim, J. Yun, J. Youm, Y. Kwon, M.-S. Kim, B. S. Kim, Y.-H. Choa, I. Cho, R. Kwak and D.-W. Jeong, *Nano Energy*, 2024, **126**, 109683.
91 A. Guchait, S. Pramanik, D. K. Goswami, S. Chattopadhyay and T. Mondal, *ACS Appl. Mater. Interfaces*, 2024, **16**, 46844–46857.
92 Y. Zhang, S. Guo, Z. G. Yu, H. Qu, W. Sun, J. Yang, L. Suresh, X. Zhang, J. J. Koh and S. C. Tan, *Adv. Mater.*, 2022, **34**, 2201228.
93 P. Li, Y. Hu, H. Wang, T. He, H. Cheng and L. Qu, *Nat. Commun.*, 2025, **16**, 6600.
94 Y. Chen, C. Ye, J. He, R. Guo, L. Qu and S. Tang, *Energy Environ. Sci.*, 2025, **18**, 6063–6075.
95 Y. Hu, W. Yang, W. Wei, Z. Sun, B. Wu, K. Li, Y. Li, Q. Zhang, R. Xiao, C. Hou and H. Wang, *Sci. Adv.*, 2024, **10**, eadk4620.
96 W. Gao, F. Liu, Y. Zheng, C. Wang, Y. Jian, J. Ju, W. Wang, Z. Lu and Y. Qiao, *Small*, 2025, **21**, 2409438.
97 S. Yang, L. Zhang, J. Mao, J. Guo, Y. Chai, J. Hao, W. Chen and X. Tao, *Nat. Commun.*, 2024, **15**, 3329.
98 X. Shi, Y. Wei, B. Tang, Y. Li, L. Lv, S. Lin, S. Luo, T. Wang, S. Tan, Q. Sun, X. Wang, X. Zheng, Y. Guo, F. Liang, W. Huang and H.-D. Yu, *Adv. Funct. Mater.*, 2025, **35**, 2419753.
99 G. Liu, Z. An, Y. Lu, Y. Wu, Z. Shi, X. Li, J. Lv, H. Wen, Z. Peng, R. P. S. Han, Y. He, Q. Ye, Q. Chen, F. Zhang, J. Liu and Q. Liu, *Nano Energy*, 2024, **119**, 109098.
100 L. Li, Z. Chen, M. Hao, S. Wang, F. Sun, Z. Zhao and T. Zhang, *Nano Lett.*, 2019, **19**, 5544–5552.
101 Y. Guo, X.-S. Zhang, Y. Wang, W. Gong, Q. Zhang, H. Wang and J. Brugger, *Nano Energy*, 2018, **48**, 152–160.
102 X. Pu, M. Liu, X. Chen, J. Sun, C. Du, Y. Zhang, J. Zhai, W. Hu and Z. L. Wang, *Sci. Adv.*, 2017, **3**, e1700015.
103 R. Xu, L. Qu and M. Tian, *Soft Matter*, 2021, **17**, 9014–9018.
104 S. Chen, H. Xia and Q.-Q. Ni, *Adv. Electron. Mater.*, 2021, **7**, 2100222.
105 K. Gao, J. Sun, X. Lin, Y. Li, X. Sun, N. Chen and L. Qu, *J. Mater. Chem. A*, 2021, **9**, 24488–24494.
106 F. Chen, S. Zhang, P. Guan, Y. Xu, T. Wan, C. H. Lin, M. Li, C. Wang and D. Chu, *Small*, 2023, **20**, 2304572.
107 S. Shen, X. Xiao, X. Xiao and J. Chen, *ACS Appl. Energy Mater.*, 2022, **5**, 3952–3965.
108 J. Bai, Y. Huang, H. Wang, T. Guang, Q. Liao, H. Cheng, S. Deng, Q. Li, Z. Shuai and L. Qu, *Adv. Mater.*, 2022, **34**, 2103897.
109 F. Chen, S. Zhang, P. Guan, Y. Xu, T. Wan, C.-H. Lin, M. Li, C. Wang and D. Chu, *Small*, 2024, **20**, 2304572.
110 B. Saikia, M. Dey, P. Garg, R. Gogoi, R. Manik and K. Raidongia, *Chem. Eng. J.*, 2024, **497**, 154840.
111 S. Sharma and T. Mondal, *Small*, 2025, **21**, 2501722.
112 X. Xiao, X. Xiao, A. Nashalian, A. Libanori, Y. Fang, X. Li and J. Chen, *Adv. Healthcare Mater.*, 2021, **10**, 2100975.
113 G. Conta, A. Libanori, T. Tat, G. Chen and J. Chen, *Adv. Mater.*, 2021, **33**, 2007502.
114 E. Brusa, A. Carrera and C. Delprete, *Actuators*, 2023, **12**, 457.
115 M. Lee, J. R. Renshof, K. J. van Zeggeren, M. J. A. Houmes, E. Lesne, M. Šiškins, T. C. van Thiel, R. H. Guis, M. R. van Blankenstein, G. J. Verbiest, A. D. Caviglia, H. S. J. van der Zant and P. G. Steeneken, *Adv. Mater.*, 2022, **34**, 2204630.
116 J. Hu, S. Liu, Y. Huo, B. Yang, Y. Yin, M. L. Tan, P. Liu, K. Cai and W. Ji, *Adv. Mater.*, 2025, **37**, 2417409.
117 Q. Hu, Y. Zhang, X. Rao, L. Wang, L. Gao, F. Li, H. Shen, L. Pan and B.-L. Hu, *Nano Lett.*, 2025, **25**, 9646–9653.
118 R. Mondal, M. A. M. Hasan, J. M. Baik and Y. Yang, *Mater. Today*, 2023, **66**, 273–301.

119 Y. Wang, H. Ye, P. Wang, Z. Wu, Q. Guan, C. Zhang, H. Li, S. Chen and J. Luo, *Adv. Mater.*, 2024, **36**, 2409245.
120 L. Xu, G. Huangfu, Y. Guo and Y. Yang, *Research*, 2023, **6**, 0028.
121 H. Ryu and S. W. Kim, *Small*, 2019, **17**, 1903469.
122 S. Zang, J. Chen, Y. Yamauchi, S. W. Sharshir, H. Huang, J. Yun, L. Wang, C. Wang, X. Lin, S. Melhi, M. Kim and Z. Yuan, *ACS Nano*, 2024, **18**, 19912–19930.